Quantitative Measurement Technique for Transcription Factor Profiles

Zuyi (Jacky) Huang, Fatih Senocak, Arul Jayaraman and Juergen Hahn
Department of Chemical Engineering
Texas A& M University
College Station, TX 77843-3122

Introduction

Control of gene expression by transcription factors is an integral component of cell signaling and gene expression regulation (Hoffmann et al., 2007). Different transcription factors exhibit different expression and activation dynamics, and together govern the expression of specific genes and cellular phenotypes (Grove and Walhout, 2008). An important requirement for the development of these signal transduction models is the ability to quantitatively describe the activation dynamics of transcriptions so that parameters can be estimated for model development. The activation of transcription factors under different conditions have been conventionally monitored using protein binding techniques such as electrophoretic mobility shift assay or chromatin immunoprecipitation (Elnitski et al., 2006). While these techniques provide snapshots of activation at a small set of single time points, they can yield only qualitative or semi-quantitative data at best. This approach also requires the use of multiple cell populations for each time point at which transcription factor activation is to be measured, and often, the true dynamics of transcription factors are not captured due to limited sampling points and frequencies. Hence, these methods are not ideal for investigating time-dependent activation of transcription factors in a quantitative manner.

More recently, fluorescence-based reporter systems have been developed for continuous and non-invasive monitoring of transcription factors and elucidation of regulatory molecule dynamics. Recent studies (Thompson et al., 2004; Wieder et al., 2005, King et al., 2007) have used green fluorescent protein (GFP) as a reporter molecule for continuously monitoring activation of a panel of transcription factors, underlying the inflammatory response in hepatocytes for 24 h. These systems involve expressing GFP under the control of a minimal promoter such that GFP expression and fluorescence is observed only when a transcription factor is activated (i.e., when the transcription factor binds to its specific DNA binding sequence and induces expression from a minimal promoter). The dynamics of GFP fluorescence is used as the indicator for dynamics of the transcription factor being profiled. The primary drawback with this approach is that it does not provide direct activation rates of the transcription factors being investigated. Even though transcription factor dynamics influence GFP dynamics, the relationship between the two is non-trivial as the induction of

GFP fluorescence itself involves multiple steps (i.e., transcription of GFP mRNA, GFP protein translation, post-translational processing, etc) (Subramanian and Srienc, 1996), and not all of these steps contribute equally to regulation of GFP expression. The observed fluorescence dynamics in GFP reporter cell systems is the result of two different dynamics: (i) the dynamics of transcription factor activation by a soluble stimulus-mediated signal transduction pathway and (ii) the dynamics of GFP expression, folding, and maturation. Therefore, it is necessary to uncouple the effects of these independent systems in order to quantitatively determine transcription factor activation profiles underlying cellular phenotpyes.

In this work, we develop a strategy for determining transcription factor concentrations from fluorescence microscopy data. This technique is based upon the following steps:

1) The image analysis method based on K-means clustering and Principal Component Analysis (PCA) (Huang and Hahn, 2007) is implemented to obtain a fluorescence intensity profile from the fluorescence microscopy images.
2) Based on the model initially presented by Subramanian and Srienc (1996), a model for transcription, translation, and activation of GFP is derived to correlate transcription factor concentration with fluorescence intensity.
3) A procedure for solving an inverse problem involving the model developed in 2) and the fluorescence data derived from the image analysis from step 1) is presented. This procedure computes the transcription factor profiles from fluorescence intensity data.

The technique has been implemented to derive quantitative concentration of NF-kB from fluorescence microscopy images of hepatocytes stimulated by TNF-α with four different concentrations. Part of the derived NF-kB data is then used to develop and refine a model of the TNF-α signaling pathway. The refined model of the TNF-α signaling pathway is tested on data not used for parameter estimation and it is found that it can predict the dynamics of TNF-α signaling pathway very well.

Preliminaries

Image analysis based on K-means clustering and Principal Component Analysis (PCA)

This method distinguishes the regions of the image with similar brightness by PCA (Hotelling, 1933) and then groups them into the same cluster by K-means clustering (Kaufman and Rousseeuw, 1990). The outline of this method is shown in the following steps:

1) For each image from the time-series of images, the areas in the image representing cells where fluorescence can be seen are determined by PCA and K-means clustering.
2) Once the cell region has been determined it is possible to compute the average fluorescence intensity by the following formula:

$$I = \left(\frac{\sum_{k=1}^{N_f} I_{f,k}}{N_f} - \frac{\sum_{k=1}^{N_b} I_{b,k}}{N_b}\right)_{stimulation} \quad (1)$$

$I_{f,k}$ refers the fluorescent intensity of the k_{th} pixel in a fluorescent cell region, $I_{b,k}$ refers the fluorescent intensity of the k_{th} pixel belonging to the background, N_f is the total number of pixels in the fluorescent cell region, N_b is the total number of pixels in the background. For a RGB image, the fluorescent intensity I is defined as the sum of the values of red and green and blue of each pixel. The reason for subtracting the intensity of the pixels representing the background is to reduce measurement noise due to brightness variations.

3) The intensity for each image is combined together to get the fluorescent intensity profile for the whole set of time-series images.

Model development

Two models are involved in this work: (a) a model describing the dynamics of the proteins involved in TNF-α signaling and (b) a model describing the dynamics of the proteins of a green fluorescent protein reporter system. The first model has the TNF-α concentration as the input to the system and the output of the system is the dynamic profile of NF-kB that results from TNF-α stimulation. The second model uses the NF-kB concentration as the input and predicts the fluorescence intensity profile that can be measured. Using these two models it is possible to determine the NF-kB concentration during an experiment by solving an inverse problem of the second model. The generated data set can then be further used to adjust parameters of the first model. Figure 1 illustrates the relationship between these two models.

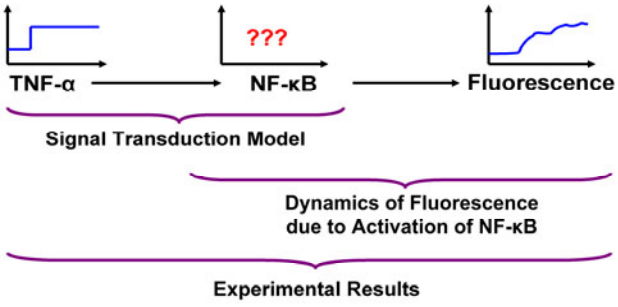

Figure 1: Relationship between input, output, and concentration of transcription factors with GFP-reporter systems.

The model describing TNF-α mediated signal transduction is shown in Figure 2 and the equations are given in 'Appendix 1'. This model is based upon the models described by Rangamani and Sirovich , 2007 and Lipniacki et al. , 2004 The model from Lipniacki et al. was used to describe signal transduction from IKKn to NF-kB whereas the model from Rangamani and Sirovich's work was used to describe signal transduction from TNF-α to IKKn. The reason for

combining these two models is that the model from Lipniacki et al.'s work does not describe signal transduction from TNF-α to IKKn, while the paper by Rangamani and Sirovich states that the signal transduction from IKKn to NF-kB as described in their model should be updated as it represents a simplification of what is currently known about the signal transduction pathway. In order to combine these two models the assumption that c-IAP in the reaction "Caspase-3*+c-IAP->caspase-3*|c-IAP" from Rangamani and Sirovich's model can be replaced with $cgen_t$ from Lipniacki et al.'s model. The rationale behind this assumption is that c-IAP and $cgen_t$ are both involved in transcription of DNA.

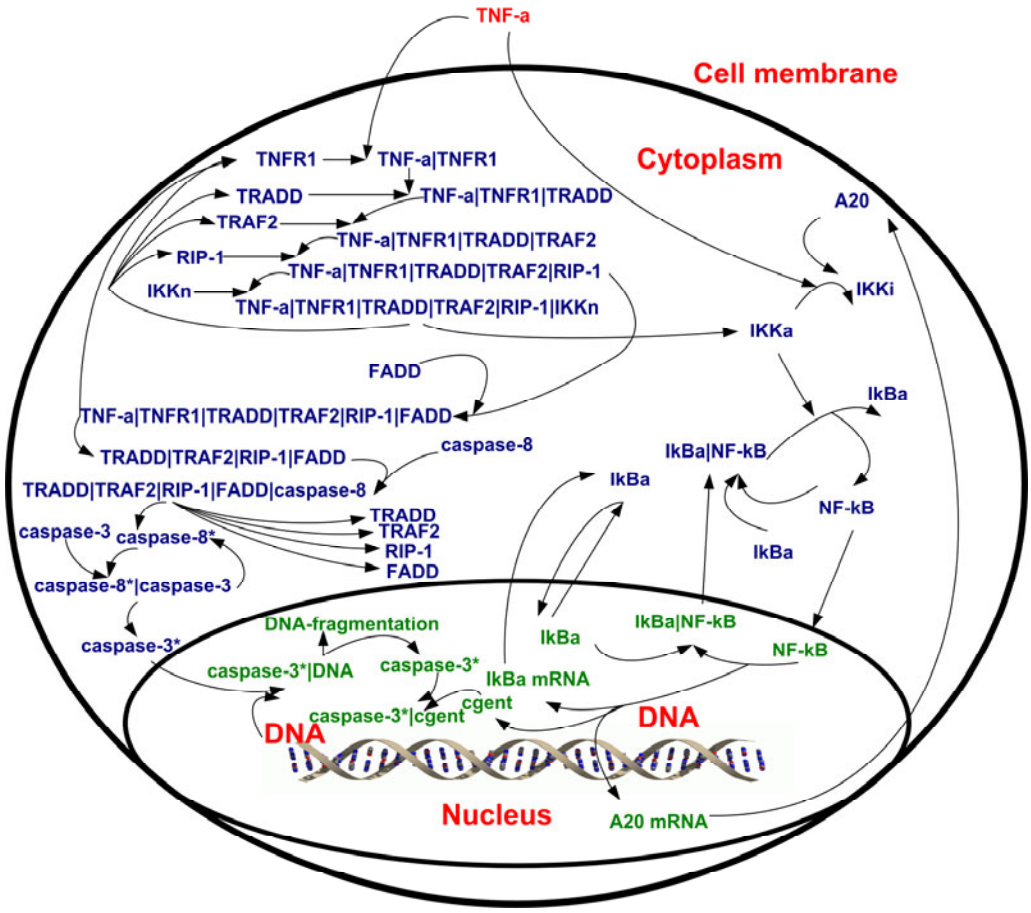

Figure 2: TNF-α signaling pathway

This integrated model, which consists of 37 differential equations and 60 parameters, can represent the dynamic behavior of the proteins involved in TNF-α-mediated NF-kB activation: TNF-α initiates the signal transduction by binding to its receptor TNFR1 and forming the complex TNF-α| TNFR1, which then recruits TRADD, TRAF2, RIP-1 to form the complex TNF-α| TNFR1|TRADD| TRAF2|RIP-1. This complex then activates two pathways: 1) it activates the apoptotic machinery by recruiting FADD; 2) it activates the NF-kB pathway by promoting the neutral form of IKK (IKKn) to the active form of IKK (IKKa). NF-kB is then released from the complex NF-kB|IkBα and translocates into the nucleus to initiate the transcription/translation process. Since the presence of NF-kB in the

nucleus (i.e., activation of NF-kB) does not immediately lead to fluorescence seen in the images it is required to augment the developed model with equation describing transcription/translation as well as activation of GFP. The equations to be added are based upon the model described by Subramanian and Srienc , 1996 , where modifications are made to account for the constant reporter DNA levels in our experiments (i.e., due to stable integration of the reporter plasmid into the genomic DNA in our reporter cell line , Thompson et al. 2004) as well as to include the effect of transcription factor concentrations on the transcription rate. These changes result in the following model describing the measurement dynamics:

$$\frac{dm}{dt} = S_m p \frac{C_{NF-\kappa B}}{C + C_{NF-\kappa B}} - D_m m \qquad (2)$$

$$\frac{dn}{dt} = S_n m - D_n n - S_f n$$

$$\frac{df}{dt} = S_f n - D_n f$$

where $C_{NF\text{-}kB}$ is the concentration of activated NF-kB in the nucleus, m is the mRNA concentration, n is the concentration of GFP, and f corresponds to the concentration of activated GFP. The values of the parameters shown in equation (2) are given in Table 1. The procedure for estimation of C is described below.
The experimental measurements consist of the fluorescence intensity, I, as seen on the images which is directly proportional to the concentration of activated green fluorescent protein:

$$f = \Delta I \qquad (3)$$

Where Δ is the ratio between activated GFP and computed fluorescence intensity.

As I can be obtained from the fluorescence images that have been processed by the image analysis procedure described in the preliminary section, the dynamics of NF-kB can be computed by solving an inverse problem involving equations (2).

Table 1 - Parameters for the model shown in equation (2).

Parameter	Value	Parameter	Value
S_m	373 1/hr	S_f	0.347 1/hr
D_m	0.45 1/hr	C	108 nM
S_n	780 1/hr	p	5 nM
D_n	0.5 1/hr	$m(0)$, $n(0)$, $f(0)$	0 nM

A procedure to get the NF-kB profile from the fluorescent intensity data by solving an inverse problem

The activation of NF-kB in H35 reporter cells was investigated by stimulating with different TNF-α concentrations (6ng/ml, 10ng/ml, 13ng/ml, and 19 ng/ml) as described in the Methods section. The data was analyzed using the described image analysis procedure, resulting in the fluorescence intensity profiles shown (red line) in Figure 3. The error bars indicated +/- one standard deviation from the mean of the measurements taken for each time point.

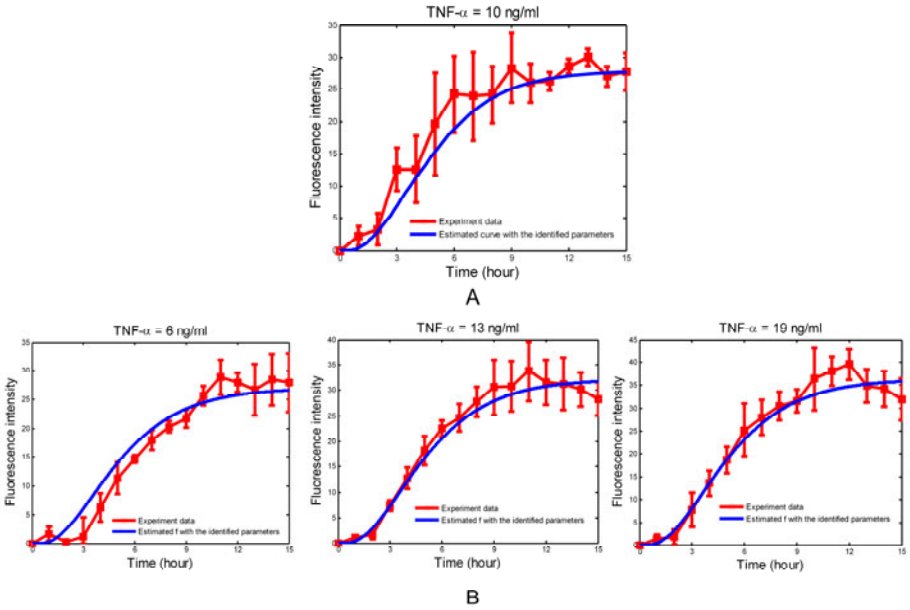

Figure 3: (A) Comparison of experimental data and the model predictions for f/Δ where the NF-kB concentration serves as the input to the model and is taken from Hoffman et al.'s paper (2002); (B) Experimental data and the fitted curve f/Δ for different TNF-α concentrations.

We developed a procedure that computes the NF-kB concentration profile from the experimental data by solving an inverse problem given by equations (2) and (3). In order to avoid a numerical solution of this inverse problem, we derived an analytical solution which computes $C_{\text{NF-kB}}$ from the fluorescence intensity profile *I*. This analytical solution treats equation (2) as a static nonlinearity

$$u = \frac{C_{\text{NF}-\kappa\text{B}}}{C + C_{\text{NF}-\kappa\text{B}}} \tag{4}$$

which is followed by a system of linear differential equations:

$$\begin{aligned} dm/dt &= S_m pu - D_m m \\ dn/dt &= S_n m - D_n n - S_f n \\ df/dt &= S_f n - D_n f \end{aligned} \tag{5}$$

Taking a Laplace transform of equation (5) results in $f(s)$ as a function of $u(s)$:

$$f(s) = \frac{S_f}{s + D_n} \cdot \frac{S_n}{s + D_n + S_f} \cdot \frac{S_m p}{s + D_m} u(s) \tag{6}$$

While it is possible to choose any function to describe $u(s)$, we opted for

$$u(s) = \frac{\omega_n^2}{s^2 + 2\varepsilon\omega_n s + \omega_n^2} \cdot \frac{T_\alpha}{s} \tag{7}$$

as $u(s)$ represents a concentration profile of $C_{\text{NF-kB}}$ that shows damped oscillatory behavior as has been reported in the literature (Hoffmann et al, 2002). Substituting equation (7) into equation (6) and performing an inverse Laplace transform results in:

$$f(t) = A_1 + A_2 e^{-D_n t} + A_3 e^{-(D_n + S_f)t} + A_4 e^{-D_m t} + A_7 e^{-\varepsilon\omega_n t} \sin(\omega_n \sqrt{1-\varepsilon^2}\, t + \varphi) \tag{8}$$

where A_1, A_2, A_3, A_4, A_7, and φ are constants with the values given in 'Appendix 2'. The values of the parameters ε, ω_n and T_α are estimated by fitting $f(t)$ to the experimental data for each experiment. The concentration of NF-kB is then given by:

$$C_{\text{NF-}\kappa\text{B}} = \frac{CT_\alpha \sqrt{1-\varepsilon^2} - CT_\alpha e^{-\varepsilon\omega_n t} \sin(\omega_n \sqrt{1-\varepsilon^2}\, t + \phi)}{(1 - T_\alpha)\sqrt{1-\varepsilon^2} + T_\alpha e^{-\varepsilon\omega_n t} \sin(\omega_n \sqrt{1-\varepsilon^2}\, t + \phi)} \tag{9}$$

, where

$$\phi = \arctan \frac{\sqrt{1-\varepsilon^2}}{\varepsilon}$$

The values of C from equation (4) and Δ from equation (3) only need to be estimated once and can be assumed to be constant for all future experiments. We have chosen the concentration profile for NF-kB as reported in the paper by Hoffman et al., 2002, which corresponds to a stimulation with 10 ng/ml of TNF-α, as the input, and have estimated C and Δ from experimental data that we have collected for stimulation with 10 ng/ml of TNF-α. The value of C was determined to be 108 nM and Δ was found to be equal to 2.5562×10^4. It should be noted that some of the data derived from a stimulation with 10 ng/ml of TNF-α was used for determining these parameter values, while other data points will be used for testing model. Figure 3A shows the fit of equation (11) to the data generated by this experiment.

Figure 3B depicts the experimental data for stimulation with 6 ng/ml, 13 ng/ml, and 19 ng/ml of TNF-α as well as the results of the system identification using equation (8). The values for C and Δ are constant for these experiments, however, the values for ε, ω_n and T_α are estimated separately for each data set. The corresponding concentration profiles for NF-kB, as computed by equation (9) are shown in Figure 4. It can be seen that stimulation with higher concentrations of TNF-α results in larger long-term concentrations of NF-kB as well as in higher peak concentrations. One important aspect of this procedure is that the data obtained is quantitative (i.e., numerical values of the NF-kB profile at each time point are obtained) and not merely qualitative.

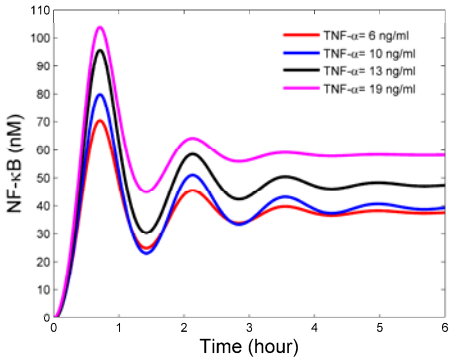

Figure 4: NF-kB profiles computed via solution of the inverse problem for TNF-α concentrations of 6 ng/ml, 10 ng/ml, 13 ng/ml, and 19 ng/ml.

These results for stimulation with 6 ng/ml, 13 ng/ml, and 19 ng/ml of TNF-α were used to estimate parameters of the signal transduction pathway model. Since the developed model contains many more parameters than can be estimated from three time series of data, it was required to use local sensitivity analysis to determine which parameters should be re-estimated. It was determined that the parameters c_3, k_{1p}, and k_r are good candidates for estimation. Nonlinear least square routines in MATLAB were then used to estimate these three parameters. The estimated values were found to be 0.0104, 0.0740 and 2.50, respectively. Since the data derived from the stimulation with 10 ng/ml of TNF-α was not used for estimating these parameters, this data set can be used for validating the accuracy of the updated model. Figure 5 shows the model prediction for 10 ng/ml of TNF-α together with the experimental results derived from the described image analysis procedure. It can be concluded that the updated model predicts experimental data very well.

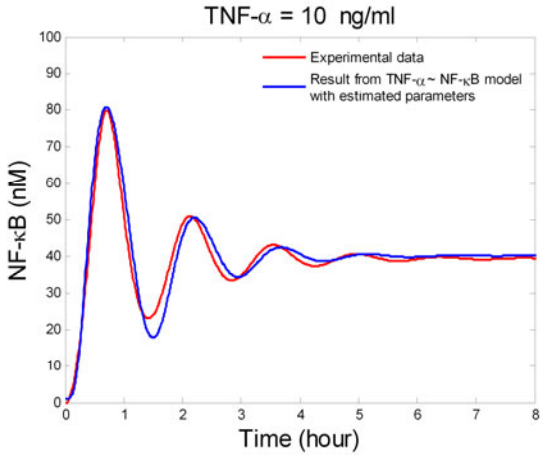

Figure 5: Comparison between NF-kB profiles computed via the presented technique for 10 ng/ml of TNF-α and simulation of the model where some parameters have been re-estimated.

Discussion and conclusion

In this study, we have demonstrated that transcription factor activation profiles can be quantitatively extracted from fluorescence reporter data. The proposed approach was effective in deriving transcription factor activation rates from GFP profiles generated from NF-kB reporter cells stimulated with 10 – 50 ng/mL of TNF-α, a concentration range that is commonly used in cell culture experiments (Damelin et al., 2007; King et al., 2007) and reported to result in strong activation of NF-kB (Wieder et al., 2005). However, predicting NF-kB activation at lower concentrations of TNF-α(< 10 ng/mL) was not as effective due to low levels of GFP signal. This is evident from Figure 3B which shows a better correlation between the model and experimental data at higher (13 and 19 ng/mL) than at lower (6 ng/mL) TNF-α concentrations. Therefore, while our method is effective for moderate-to-high levels of activation, further improvement (e.g., in the image analysis methods) is needed to increase the GFP signal/noise ratio for effectively predicting profiles of low abundance transcription factors.

Another discrepancy between the model and experimental data is predicting long-term NF-kB activation profiles. The data in Figure 3B shows that fluorescence decreases after ~ 11 h even though the stimulus (TNF-α) is continually present, with the decrease being more pronounced at the higher concentrations. However, this decrease is not reflected in Figure 3B which shows NF-kB levels being constant beyond 11 h as the assumed model structure from equation (7) cannot represent this decrease. It is possible to postulate a different profile for the transcription factor, resulting in differences in equation (7), e.g., one that can reflect such a decrease. However, it is not clear if the decrease in fluorescence observed after ~ 11 h of stimulation results from experimental artifacts (i.e., fluorescence photobleaching and cell death arising from cells being repeatedly exposed to UV light for imaging) or is a real biological phenomenon (i.e., consequence of change in gene expression arising due to constant stimulation with TNF-α). A better understanding of long-term activation is needed to evaluate this behavior.

In summary we have developed a methodology for quantitatively determining transcription factor profiles. This technique makes use of fluorescence microscopy images from a GFP reporter system for transcription factor activation and involves solving an inverse problem to determine the transcription factor profile from the fluorescence intensity dynamics. Data generated by this method can then be used to estimate parameters for signal transduction pathway models. This technique was applied to the activation of NF-kB by TNF-α, however, it can be used to determine transcription factor profiles for any system where limited qualitative knowledge about the transcription factor dynamics exists.

References

Damelin. LH., S. Coward, M. Kirwan, P. Collins, C. Selden, HJF. Hodgson (2007). “Fat-loaded HepG2 spheroids exhibit enhanced protection from Pro-oxidant and cytokine induced damage.” J Cell Biochem, 101:723-734.

Elnitski, L., V. X. Jin, P. J. Farnham and S. J. Jones (2006). "Locating mammalian transcription factor binding sites: a survey of computational and experimental techniques." Genome Res 16, 1455-1464.

Grove, C. A. and A. J. M. Walhout (2008). “Transcription factor functionality and transcription regulatory networks.” Molecular Biosystems, 4: 309-314.

Hotelling, H (1933). “Analysis of a Complex of Statistical Variables into Principal Components.” Journal of Educational Psychology, 24, 417-441.

Hoffmann, A, A. Levchenko, M.L. Scott, and D. Baltimore (2002). “The IkB–NF-kB signaling module: temporal control and selective gene activation.” Science, 298(8), 1241-1245.

Huang, Z and J. Hahn (2007). “Development and Comparison of Algorithms for Analysis of Fluorescent Images for Studying the Dynamics of Signal Transduction Pathways.” AIChE Annual Conference at Salt Lake City, 2007.

Kaufman, L. and P. J. Rousseeuw (1990). “Finding Groups in Data: an Introduction to Cluster Analysis.” John Wiley & Sons Press.

King, K.R., S. Wang, D. Irimia, A. Jayaraman, M. Toner, M.L. Yarmush (2007). “A high-throughput microfluidic real-time gene Expression living cell array.” Lab Chip 7, 77-85.

Lipniacki, T., P. Paszek, A.R. Brasier, B. Luxon, and M. Kimmel (2004). “Mathematical model of NF-kB regulatory module.” Journal of Theoretical Biology 228, 195–215.

Rangamani, P. and L. Sirovich (2007). “Survival and apoptotic pathways initiated by TNF-α: modeling and predictions.” Biotechnology & Bioengineering 97(5), 1216-1229.

Subramanian, S. and F. Srienc (1996). “Quantitative analysis of transient gene expression in mammalian cells using the green fluorescent protein.” J. Biotechnol. 49, 137-151.

Thompson, D. M., K. R. King, K. J. Wieder, M. Toner, M. L. Yarmush and A. Jayaraman (2004). "Dynamic gene expression profiling using a microfabricated living cell array." Anal Chem 76, 4098-4103.

Wieder, KJ., KR. King, DM. Thompson, C. Zia, ML. Yarmush, A. Jayaraman (2005). “Optimization of reporter cells for expression profiling in a microfluidic device.” Biomed Microdevices, 7:213-222.

Appendix 1

This file describes the equations, the initial values of state variables, and parameters of the model describing TNF-α mediated signal transduction

$$\dot{x}_1 = -k_{1p}x_1u + k_{2p}x_2 + k_{17p}x_{26} + k_{11p}x_{10}$$
$$\dot{x}_2 = k_{1p}x_1u - k_{2p}x_2 - k_{3p}x_2x_3 + k_{4p}x_4$$
$$\dot{x}_3 = -k_{3p}x_2x_3 + k_{4p}x_4 + k_{11p}x_{10} + k_{20p}x_{29}$$
$$\dot{x}_4 = k_{3p}x_2x_3 - k_{4p}x_4 - k_{5p}x_4x_5 + k_{6p}x_6$$
$$\dot{x}_5 = -k_{5p}x_4x_5 + k_{6p}x_6 + k_{11p}x_{10} + k_{20p}x_{29}$$
$$\dot{x}_6 = k_{5p}x_4x_5 - k_{6p}x_6 - k_{7p}x_6x_7 + k_{8p}x_8$$
$$\dot{x}_7 = -k_{7p}x_6x_7 + k_{8p}x_8 + k_{11p}x_{10} + k_{20p}x_{29}$$
$$\dot{x}_8 = k_{7p}x_6x_7 - k_{8p}x_8 - k_{9p}x_8x_9 + k_{10p}x_{10} - k_{15p}x_8x_{25} + k_{16p}x_{26}$$
$$\dot{x}_9 = -k_{9p}x_8x_9 + k_{10p}x_{10} + k_{14p}x_{14}$$
$$\dot{x}_{10} = k_{9p}x_8x_9 - k_{10p}x_{10} - k_{11p}x_{10}$$
$$\dot{x}_{11} = k_{11p}x_{10} - k_3x_{11} - T_R k_2 x_{11}x_{17} - k_{deg}x_{11} - a_2x_{11}x_{19} + t_1x_{13} - a_3x_{11}x_{22} + t_2x_{14}$$
$$\dot{x}_{12} = k_3x_{11} + T_R k_2 x_{11}x_{17} - k_{deg}x_{12}$$
$$\dot{x}_{13} = a_2x_{11}x_{19} - t_1x_{13}$$
$$\dot{x}_{14} = a_3x_{11}x_{22} - t_2x_{14}$$
$$\dot{x}_{15} = c_{6a}x_{22} - a_1x_{15}x_{19} + t_2x_{14} - i_1x_{15}$$
$$\dot{x}_{16} = i_1k_v x_{15} - a_1x_{20}x_{16}$$
$$\dot{x}_{17} = c_4x_{18} - c_5x_{17}$$
$$\dot{x}_{18} = c_2 + c_1x_{16} - c_3x_{18}$$
$$\dot{x}_{19} = -a_2x_{11}x_{19} - a_1x_{19}x_{15} + c_{4a}x_{21} - c_{5a}x_{19} - i_{1a}x_{19} + e_{1a}x_{20}$$
$$\dot{x}_{20} = -a_1x_{16}x_{20} + i_{1a}k_v x_{19} - e_{1a}k_v x_{20}$$
$$\dot{x}_{21} = c_{2a} + c_{1a}x_{16} - c_{3a}x_{21}$$
$$\dot{x}_{22} = a_1x_{19}x_{15} - c_{6a}x_{22} - a_3x_{11}x_{22} + e_{2a}x_{23}$$
$$\dot{x}_{23} = a_1x_{20}x_{16} - e_{2a}k_v x_{23}$$
$$\dot{x}_{24} = c_{2c} + c_{1c}x_{16} - c_{3c}x_{24} - k_{28p}x_{24}x_{33}$$
$$\dot{x}_{25} = -k_{15p}x_8x_{25} + k_{16p}x_{26} + k_{20p}x_{29}$$
$$\dot{x}_{26} = k_{15p}x_8x_{25} - k_{16p}x_{26} - k_{17p}x_{26}$$
$$\dot{x}_{27} = k_{17p}x_{26} - k_{18p}x_{27}x_{28} + k_{19p}x_{29}$$
$$\dot{x}_{28} = -k_{18p}x_{27}x_{28} + k_{19p}x_{29}$$
$$\dot{x}_{29} = k_{18p}x_{27}x_{28} - k_{19p}x_{29} - k_{20p}x_{29}$$
$$\dot{x}_{30} = k_{20p}x_{29} - k_{21p}x_{30}x_{31} + k_{22p}x_{32} + k_{23p}x_{32}$$
$$\dot{x}_{31} = -k_{21p}x_{30}x_{31} + k_{22p}x_{32}$$
$$\dot{x}_{32} = k_{21p}x_{30}x_{31} - k_{22p}x_{32} - k_{23p}x_{32}$$
$$\dot{x}_{33} = k_{23p}x_{32} - k_{28p}x_{24}x_{33} - k_{24p}x_{33}x_{36} + k_{25p}x_{37} + k_{26p}x_{37}$$
$$\dot{x}_{34} = k_{26p}x_{37}$$
$$\dot{x}_{35} = k_{28p}x_{24}x_{33}$$
$$\dot{x}_{36} = -k_{24p}x_{33}x_{36} + k_{25p}x_{37}$$
$$\dot{x}_{37} = k_{24p}x_{33}x_{36} - k_{25p}x_{37} - k_{26p}x_{37}$$
$$y = x_{16} / k_r$$

State variables of the model and their initial values:

Name	Species	Initial values (μM)
x_1	TNFR1	0.1
x_2	TNF-α/TNFR	0
x_3	TRADD	0.15
x_4	TNF-α/TNFR1/TRADD	0
x_5	TRAF2	0.1
x_6	TNF-α/TNFR1/TRADD/TRAF2	0
x_7	RIP-1	0.1
x_8	TNF-α/TNFR1/TRADD/TRAF2/RIP-1	0
x_9	IKKn	0.2
x_{10}	TNF-α/TNFR1/TRADD/TRAF2/RIP-1/IKKn	0
x_{11}	IKKa	0
x_{12}	inactive IKK	0
x_{13}	cytoplasmic IKK|IkBa complex	0
x_{14}	cytoplasmic IKK|IkBa|NF-kB complex	0
x_{15}	free cxtoplasmic NF-kB	0.0003
x_{16}	free nuclear NF-kB	0.0023
x_{17}	cytoplasmic A20	0.0048
x_{18}	A20 transcription	0
x_{19}	free cytoplasmic IkBa	0.0025
x_{20}	free nuclear IkBan	0.0034
x_{21}	IkB transcription	0
x_{22}	cytoplasmic IkBa|NF-kB complex	0.0592
x_{23}	Nuclear IkBa|NF-kB complex	0.0001
x_{24}	Control gene mRNA level or c-IAP	0
x_{25}	FADD	0.1
x_{26}	TNF-α/TNFR1/TRADD/TRAF2/RIP-1/FADD	0
x_{27}	TRADD/TRAF2/RIP-1/FADD	0
x_{28}	Caspase-8	0.08
x_{29}	TRADD/TRAF2/RIP-1/FADD/caspase-8	0
x_{30}	Caspase-8*	0
x_{31}	Caspase-3	0.2
x_{32}	Caspase-8*/caspase-3	0
x_{33}	Caspase-3*	0
x_{34}	DNA-fragmentation	0
x_{35}	Caspase-3*/c-IAP	0
x_{36}	DNA intact	0.8
x_{37}	Caspase-3*/DNA	0

Note: u is the concentration of TNF-α, ng/ml. The molecule weight of TNF-α is 17 kDa. The unit ng/ml can be converted to μM by dividing by 17×10^3. y is the system output NF-kB after being scaled by k_r in units of μM.

Values of the parameters

Name	Value	Name	Value
k_v	5	k_{1p}	0.0740 (0.185)
AB^*	1	k_{15p}	0.185
c_1	$5\times10^{-7}\ AB$	k_{2p}	0.00125
c_2	0	k_{16p}	0.00125
c_3	0.0104 (0.0004)	k_{3p}	0.185
c_4	0.5	k_{17p}	0.37
c_5	0.0003	k_{4p}	0.00125
k_1	0.0025	k_{18p}	0.5
k_2	0.1	k_{5p}	0.185
k_3	0.0015	k_{19p}	0.2
k_{deg}	0.000125	k_{6p}	0.00125
a_2	0.2	k_{20p}	0.1
a_1	0.5	k_{7p}	0.185
a_3	1.	k_{21p}	0.1
t_1	0.1	k_{8p}	0.00125
t_2	0.1	k_{22p}	0.06
AA^*	1	k_{9p}	0.185
c_{1a}	$5\times10^{-7}\ AA$	k_{23p}	100
c_{2a}	0	k_{10p}	0.00125
c_{3a}	0.0004	k_{24p}	0.185
c_{4a}	0.5	k_{11p}	0.37
c_{5a}	0.0001	k_{25p}	0.00125
c_{6a}	0.00002	k_{12p}	0.014
i_1	0.0025	k_{26p}	0.37
e_{2a}	0.01	k_{13p}	0.00125
i_{1a}	0.001	k_{14p}	0.37
e_{1a}	0.0005	k_{28p}	0.5
c_{1c}	5×10^{-7}	p	1.75
c_{2c}	0	T_r^*	1
c_{3c}	0.0004	k_r	2.5

* Note: 1) AA = 1 refers to wt cell, while AA = 0 refers to IkBa deficient cell
2) AB = 1 refers to wt cell, while AB = 0 refers to A20 deficient cell
3) T_r = 0 when TNF-α is off, while T_r = 1 when TNF-α is on
4) Values in brackets refer to the model fit to the experimental data

Appendix 2

Equations for computing the values of the constants found in Equation (11)

$$A_1 = S_f S_n S_m p T_a / D_n /(D_n + S_f)/ D_m$$

$$A_2 = -S_n S_m p \omega_n^2 T_a /(D_m - D_n)/(D_n^2 - 2\varepsilon\omega_n D_n + \omega_n^2)/ D_n$$

$$A_3 = S_n S_m p \omega_n^2 T_a /(D_m - D_n - S_f)/((D_n + S_f)^2 - 2\varepsilon\omega_n (D_n + S_f) + \omega_n^2)/(D_n + S_f)$$

$$A_4 = S_f S_n S_m p \omega_n^2 T_a /(D_n - D_m)/(D_m - D_n - S_f)/(D_m^2 - 2\varepsilon\omega_n D_m + \omega_n^2)/ D_m$$

$$A_5 = -C_0 d_1 /(b d_1^2 + b d_0^2)$$

$$A_6 = C_0 (a d_1 + b d_0)/(b d_1^2 + b d_0^2)$$

$$A_7 = \sqrt{A_5^2 + (\frac{A_6 - A_5 \varepsilon\omega_n}{\omega_n \sqrt{1-\varepsilon^2}})^2}$$

$$a = -\varepsilon\omega_n$$

$$b = \omega_n \sqrt{1-\varepsilon^2}$$

$$d_1 = -(a_3 + 4a)b^3 + (3a_3 a^2 + 2a_2 a + 4a^3 + a_1)b$$

$$d_0 = b^4 + a_3 a^3 - (3a_3 a + a_2 + 6a^2)b^2 + a_2 a^2 + a^4 + a_1 a$$

$$a_1 = (D_n^2 + D_n S_f) D_m$$

$$a_2 = D_n^2 + D_n S_f + 2 D_n D_m + D_m S_f$$

$$a_3 = 2D_n + D_m + S_f$$

$$C_0 = S_f S_n S_m p \omega_n^2 T_\alpha$$

$$\varphi = \arctan \frac{A_5 \omega_n \sqrt{1-\varepsilon^2}}{A_6 - A_5 \varepsilon\omega_n}$$